



Probability of Detection Functions of Polarization-MIMO Systems in Random LOS

Downloaded from: <https://research.chalmers.se>, 2025-12-05 00:13 UTC

Citation for the original published paper (version of record):

Razavi, A., Glazunov, A. (2017). Probability of Detection Functions of Polarization-MIMO Systems in Random LOS. IEEE Access, 5: 25635-25645. <http://dx.doi.org/10.1109/ACCESS.2017.2769804>

N.B. When citing this work, cite the original published paper.

© 2017 IEEE. Personal use of this material is permitted. Permission from IEEE must be obtained for all other uses, in any current or future media, including reprinting/republishing this material for advertising or promotional purposes, or reuse of any copyrighted component of this work in other works.

Received October 2, 2017, accepted October 26, 2017, date of publication November 3, 2017, date of current version December 5, 2017.

Digital Object Identifier 10.1109/ACCESS.2017.2769804

Probability of Detection Functions of Polarization-MIMO Systems in Random-LOS

AIDIN RAZAVI¹ AND ANDRÉS ALAYÓN GLAZUNOV², (Senior Member, IEEE)

¹Ericsson Research, 411 58 Gothenburg, Sweden

²Signals and Systems Department, Chalmers University of Technology, 412 96 Gothenburg, Sweden

Corresponding author: Aidin Razavi (aidin.razavi@tgeik.com)

This work was supported in part by the two projects from Sweden's Innovation Agency VINNOVA, one within the VINN Excellence Center Chase at Chalmers and another via the Program Innovative ICT 2013, and in part by internal support from Chalmers.

ABSTRACT We derive the probability of detection functions of 1- and 2-bitstreams for polarization multiple-input multiple-output antenna systems in random line-of-sight propagation conditions. The derivations are produced assuming that the angle-of-arrival of the field impinging at the receive antenna is fixed. Hence, randomness is only due to the direction of polarization of the incident field relative to the polarization of the far-field of the receiver antenna. Also, a general analytical orthogonalization transformation matrix has been derived for far-field functions of arbitrary dual-polarized antennas and used in the probability of detection derivations. Analytical results are obtained for the maximum ratio combining receiver diversity and the zero-forcing multiplexing receiver algorithms. These results provide a practical prediction tool of the impact of antennas on system performance due to polarization deficiencies of analytical, measured or simulated radiation field patterns of dual polarized antennas. This is illustrated by the provided numerical examples.

INDEX TERMS Antenna theory, MIMO, antenna measurements.

I. INTRODUCTION

The development of 5G wireless communication systems, e.g., for high throughput data transmissions, poses strict requirements on the performance of wireless devices (e.g., mobile phones, wireless transceivers in vehicles, access points and base stations), which calls for their thorough characterization. In laboratory conditions, this is done in Over The Air (OTA) measurement setups [1]. OTA characterization of devices requires among other things a good knowledge of the propagation channel in which the devices are intended to operate. Therefore, channel models are used based on extensive and accurate channel sounding measurement campaigns (see, e.g., [2], [3] for recent reports). However, they can only cover a limited number of possible *typical* propagation scenarios.

As an alternative to OTA characterization in typical propagation scenarios, the characterization in two *limiting propagation scenarios* has been proposed in [4]. The first limiting scenario is the Rich Isotropic MultiPath (RIMP) environment which represents a good model for environments with high multipath and scattering. The RIMP environment is emulated in well-stirred reverberation chambers. In a reverberation chamber the walls are reflective and a number of so-called “stirrers” move inside the chamber, scattering the waves [5].

The other limiting scenario is the (pure) Line of Sight (LOS) environment where the antennas on two sides of a link are assumed to be fixed and only one signal path is considered between the two. This environment is emulated in anechoic chambers where the walls are fitted with absorbers and the relative location and orientation of the two antennas is under precise control.

In 5G wireless systems, with ultra-dense deployment of mm-wave radio links to users, links dominated by the LOS propagation component are foreseen [6]. The electrical distance to scatterers will be larger than in current 3G and 4G systems and the losses are higher at these frequencies. However, unlike the traditional LOS scenario, the user side of this link will suffer from the random location and orientation of the users and the way they are using the terminals. A similar situation does also apply to automotive wireless communication systems in rural areas where the vehicle usually has a LOS connection to a base-station, but the orientation of the vehicle is random in the horizontal plane. The term Random Line-Of-Sight (Random-LOS) has been introduced to describe this scenario [4], [7].

The performance of an antenna in a wireless system can be statistically characterized, e.g., by using the ideal threshold receiver model [8]. Hence, for multiple-input

multiple-output (MIMO) wireless systems, the Probability of Detection (PoD) of one or more bitstreams can be evaluated. The PoD functions provide a concise and useful model of the expected relative throughput delivered to a user evaluated as MIMO efficiency.

Polarization diversity can improve the MIMO system performance when the polarization is random in pure LOS, where randomness is only due to the direction of polarization of the incident field relative to the polarization of the far-field of the receiver antenna [9], [10]. However, it has been shown recently that so-called polarization-MIMO antennas will face performance degradations in a Random-LOS environment due to polarization deficiencies which are present at off-boresight directions [11], [12]. The two ports of a dual polarized antenna, will provide orthogonal and balanced far-fields only close to boresight direction. The far-field vectors may in fact be parallel to each other in 45° planes and the gains are very much different in the symmetry planes. These two effects, namely polarization non-orthogonality and amplitude imbalance are collectively named as polarization deficiencies. They will lead to significant performance degradations in the MIMO efficiency coverage in directions away from the boresight, especially if linear polarization is used at both transmitter and receiver sides of the link. However, there are no known general closed-form equations that can be used to determine the MIMO efficiency directly from measured or simulated antenna parameters, i.e., far-field functions and radiation efficiencies. It is highly desirable to obtain such equations since the MIMO efficiency would then be obtained in a more agile manner and at the same time it would provide better understanding of the relationship between the MIMO efficiency performance degradation due to polarization deficiencies [11]. The current manuscript fills this knowledge gap.

In this paper, we focus on the MIMO efficiency in the pure LOS environment, i.e., no multipath contribution due to scattering at all. Hence, maximum two orthogonal polarizations can be achieved in the far-field, and therefore also maximum two bitstreams are considered. The contributions of the present paper can be summarized as follows: (i) we derive analytical expressions for the PoD of 1-bitstream and 2-bitstream MIMO systems in a Random-LOS environment, assuming linear polarized antennas. These analytical formulas can be used to specifically determine the PoD of MRC SIMO and ZF MIMO systems without the need to run potentially complex and time-consuming simulations, (ii) they can also help determine the degradations in the system performance due to polarization deficiencies [11], [13], (iii) examples illustrating the throughput coverage of known antennas obtained with the analytical PoD functions are provided, and (iv) a transformation matrix has been derived for arbitrary antennas to produce orthogonal far-field functions and maximum receive power in Random-LOS, which provides a generalization of sum and difference far-field functions.

The assumed MIMO receiver model and algorithms are described in Sec. II, the considered Random-LOS channel

model is given in Sec. III, analytical results for the orthogonalization of the far-field functions are given in Sec. IV, followed by the derived analytical PoD functions in Sec. V, the numerical examples and the conclusions are given in Sec. VI and VII, respectively. Sketches of the analytical derivations are given in the Appendices.

II. MIMO RECEIVER MODEL AND RECEIVER ALGORITHMS

A. MIMO RECEIVER ALGORITHMS

In LOS, which is the focus of this paper, maximum two independent polarizations are possible. Hence, maximum number of considered antennas at both the transmitter and receiver sides is 2. In a generic MIMO system the signals received by a multi-port antenna can be expressed by the following input-output relationship

$$\mathbf{y} = \mathbf{H}\mathbf{x} + \mathbf{n} \quad (1)$$

where $\mathbf{y} \in \mathbb{C}^{N_r \times 1}$ denotes a vector of the received signals, $\mathbf{x} \in \mathbb{C}^{N_t \times 1}$ is a vector containing the transmitted signals, $\mathbf{H} \in \mathbb{C}^{N_r \times N_t}$ is the MIMO channel matrix, and $\mathbf{n} \in \mathbb{C}^{N_r \times 1}$ is the noise vector containing independent identically distributed (i.i.d.) unit variance Gaussian-distributed elements. N_r and N_t denote the number of receive and transmit antennas, respectively. The elements of the channel matrix \mathbf{H} are proportional to the induced voltages at the ports of the receiver antenna.

As well-known, the number of maximum parallel data streams that can be obtained is given by $\min\{N_r, N_t\}$. Since we are concerned with Polarization-MIMO in Random-LOS, SIMO and MIMO systems are reduced to the analysis of 1- and 2-bitstream MIMO systems.

We now specialize our results to three specific cases corresponding to algorithms used in practice in wireless communications systems. Next, we recall the receive SNR at the output of the receiver after the signal processing.

1) 1-BITSTREAM SISO SYSTEM

In this case we have a single transmit antenna and a single receive antenna, i.e., $N_r = N_t = 1$. The output SNR is then given by

$$\gamma^{\text{SISO}} = |h|^2 \gamma_t \quad (2)$$

where h is the only element of the channel matrix \mathbf{H} and $\gamma_t = E[|x|^2] / E[|n|^2]$ is proportional to the transmit power.

2) 1-BITSTREAM MRC SIMO DIVERSITY SYSTEM

The same transmitted data stream is received at two antennas, i.e., $N_t = 1$ and $N_r = 2$. The received power is maximized by using the maximum ratio combining (MRC) algorithm. The output SNR at the receiver is then given by

$$\gamma^{\text{MRC}} = \sum_{i=1}^{N_r} |h_i|^2 \gamma_t \quad (3)$$

where $\gamma_i = E[|x_i|^2]/E[|n_i|^2]$, where we have used that $E[|n_i|^2] = E[|n|^2]$ for $i = \{1, 2\}$.

3) 2-BITSTREAM ZF-MIMO OPEN LOOP MULTIPLEXING SYSTEM

Two parallel data bitstreams are transmitted and received, i.e., $N_r = N_t = 2$. No channel state information is available at the transmitter. The Zero-Forcing (ZF) algorithm applies an inversion of the channel matrix to nullify the interference from the other data bitstream. The SNR of the i -th data stream is then obtained as

$$\gamma_i^{\text{ZF}} = \frac{\gamma_i}{\left[(\mathbf{H}^H \mathbf{H})^{-1} \right]_{i,i}} \quad (4)$$

where, $\gamma_i = E[|x_i|^2]/2E[|n_i|^2]$ and $[\mathbf{X}]_{i,i}$ the i -th diagonal element of the matrix \mathbf{X} for $i = \{1, 2\}$. \mathbf{X}^{-1} denotes the matrix inversion operation.

B. IDEAL DIGITAL THRESHOLD RECEIVER

It has been shown in [8] that the data throughput in LTE (Long Term Evolution) and LTE-A (LTE-Advanced) systems can be modelled by the ideal digital threshold receiver model. This receiver assumes an ideal error correction of the transmitted information bits over an AWGN (Additive White Gaussian Noise Channel) channel. A threshold Signal-to-Noise Ratio (SNR), γ_{th} , is defined such that a signal is detected if the received SNR, γ , is above this threshold value. On the other hand, if the received SNR is below the threshold, no data is decoded at the receiver. Hence, in the static channel, when $\gamma = \gamma_{\text{th}}$, the data throughput goes sharply from 0 to the maximum achievable throughput defined by the coding and modulation scheme according to the standard specification value $T_{\text{put,max}}$.

In a dynamic fading channel the normalized average data throughput, T_{put} , can be modelled by the probability of detection of a single data bitstream

$$\text{PoD} = \frac{T_{\text{put}}}{T_{\text{put,max}}} = 1 - F(\gamma_{\text{th}}) \quad (5)$$

where $F(\gamma)$ denotes the Cumulative Distribution Function (CDF) of the average SNR after digital processing [8]. Hence, (5) denotes the complimentary cumulative distribution function of the receive SNR over the fading channel.

It is worthwhile to note that for practical OTA applications, e.g., when computing or measuring the PoD (relative throughput), power quantities are usually used instead of SNR quantities. Hence, it is often convenient to use transmit power P_t and receiver threshold power P_{th} instead of γ_t and γ_{th} , respectively. Clearly, since we consider systems with fixed noise variance the SNR ratios will be equal to power ratios. Throughout this paper we therefore use SNR quantities. In this paper we evaluate the probability of detection as $\text{PoD}\left(\frac{\gamma_t}{\gamma_{\text{th}}}\right)$. Moreover, when we say transmit SNR, we mean transmit power divided by the noise power at the receiver.

For 1-bitstream systems like the SISO and the MRC SIMO system the PoD is then directly obtained from the evaluation of the received signal SNR. On the other hand, for the ZF MIMO system, the input to the ideal digital threshold receiver is given by

$$\gamma^{\text{ZF}} = \min(\gamma_1^{\text{ZF}}, \gamma_2^{\text{ZF}}) \quad (6)$$

where the weakest of the bitstreams, i.e., the bitstream with the smallest SNR, is selected at the output of the MIMO receiver antenna. This is because the weakest performing bitstream is the one which limits the performance of the 2-bitstream system. As soon as the PoD on this stream is reduced to zero, the system is effectively a 1-bitstream system. γ_i^{ZF} for $i = \{1, 2\}$ denotes the SNR of each bitstream at the output of the ZF MIMO receiver. The PoD is then obtained using the relationship (5). Clearly, if the weakest data stream is detected, i.e., its SNR is above the threshold, then both bitstreams will be detected in a 2-bitstream MIMO system [14]. Furthermore, (5) can be used to find the required SNR to achieve 95% PoD level. The SNR relative to threshold at 95% PoD is a measure of system's performance and its degradation corresponds to the MIMO efficiencies defined in [11] for Random-LOS environments.

III. CHANNEL MODEL

Considering that our antennas are operating in a pure line-of-sight (LOS) channel, the elements of the channel matrix in (1) are proportional to the open-circuit voltage induced at the receive antenna ports by the impinging LOS wave [15]

$$V_{\text{oc},ij} = \frac{2\lambda}{j\eta I_i} \mathbf{G}_i \cdot \mathbf{E}_j \quad (7)$$

where η is the free space wave impedance, λ is the wavelength, \mathbf{G}_i is the embedded far-field function¹ of the receive antenna i in the direction $\hat{\mathbf{r}}_0$. \mathbf{G}_i is obtained on transmit when the impressed current at the input port is I_i and the other port is terminated in 50Ω . Hence, \mathbf{G}_i already takes into account the mutual coupling effects between the two receive antennas in the SIMO and MIMO cases. The direction of polarization is given by vector $\hat{\mathbf{g}}_i$, i.e., the unit vector of $\hat{\mathbf{G}}_i$. \mathbf{E}_j is the incident plane wave field with polarization vector $\hat{\mathbf{e}}_j$ measured at the phase center of the receive antenna that we choose to be the origin of the coordinate system associated with the antenna. The indices i and j can take on values $\{1, 2\}$ in the general MIMO case, while for the SISO case, $i = j = 1$, and for the SIMO case we have $i = \{1, 2\}$ and $j = 1$.

In the SIMO and MIMO cases the two receive antennas are identical. Hence, the patterns of the two antennas are identical too, while they are rotated with respect to each other and have coinciding phase centers. We assume the antennas to be terminated with conjugate-matched load condition.

¹It is worthwhile to note that bold vector notation is used to denote the far-field functions $\mathbf{G}(\theta, \phi)$. They shall not be confused with gain $G_o(\theta, \phi)$. We follow the notation introduced in [15].

Hence, we model the (ij) entry of the channel matrix in (1) as

$$h_{ij} = \frac{V_{oc,ij}}{2\sqrt{2R_a p_{ij}^{iso}}} \quad (8)$$

where R_a is the real part of the receive antenna input impedance and

$$p_{ij}^{iso} = \frac{\pi |E_j|^2}{2\eta k^2} \quad (9)$$

is the power that would have been received by an isotropic antenna that is polarization-matched to the incident field E_j . It is worthwhile to note that (8) is dimensionless.

Now, taking into account (1), (7), (8) and (9) we summarize the channel matrix entries in LOS for each considered case.

SISO System:

$$h = \sqrt{G_o} \hat{g} \cdot \hat{e} \quad (10)$$

where G_o is the gain of the receive antenna evaluated at the AoA of the LOS wave, \hat{g} and \hat{e} are the polarization vectors of the receive antenna and the LOS wave, respectively.

1 × 2 SIMO System:

$$h_i = \sqrt{G_{o,i}} \hat{g}_i \cdot \hat{e} \quad (11)$$

where $G_{o,i}$ is the gain of the receive antenna i evaluated at the AoA of the LOS wave, \hat{g}_i and \hat{e} are the polarization vectors of the receive antenna i and the LOS wave, respectively.

2 × 2 MIMO System:

$$h_{ij} = \sqrt{G_{o,i}} \hat{g}_i \cdot \hat{e}_j \quad (12)$$

where $G_{o,i}$ is the gain of the receive antenna i evaluated at the AoA of the LOS waves, \hat{g}_i and \hat{e}_j are the polarization vectors of the receive antenna i and the LOS wave j , respectively. It is worthwhile to note that in our case

$$\hat{e}_j \cdot \hat{e}_{j'}^* = \delta_{jj'} \quad (13)$$

which means that for the sake of simplicity we assume that the transmit waves are orthogonally polarized.

Under the above assumptions it is clear that the polarization mismatch between the receive antenna (or antennas) and the impinging field can be characterized by an angle ψ

$$|\hat{g} \cdot \hat{e}|^2 = \cos^2(\psi) \quad (14)$$

where ψ is assumed uniformly distributed in $[0, \pi/2]$ with probability distribution

$$f_\psi(\psi) = \frac{2}{\pi}, \quad 0 \leq \psi \leq \frac{\pi}{2}. \quad (15)$$

It is worthwhile to note that (15) is a hypothetical distribution. In practice, the distribution might not necessarily be uniform, but no other models are currently available. However, the choice of the uniform distribution is a result of the nature of the Random-LOS as a limiting scenario. In the SIMO and MIMO cases, and following the notation introduced above, the polarization mismatch angle can be denoted by ψ . Hence, in the following we use this model where no special preference exists for any polarization state of the waves impinging at the receive antenna.

IV. ANTENNA FAR-FIELD ORTHOGONALIZATION

As mentioned above, the far-field functions $G_1(\theta_0, \phi_0)$ and $G_2(\theta_0, \phi_0)$ of dual polarized receive antennas are not orthogonal in all AoA directions defined by spherical angles (θ_0, ϕ_0) . However, for further derivations of PoD functions, it is convenient to obtain two replacement vectors G_Σ and G_Δ that are orthogonal, i.e.

$$G_\Sigma \cdot G_\Delta^* = 0 \quad (16)$$

and provide the same MRC gain as the above, i.e.

$$|G_1 \cdot E_i|^2 + |G_2 \cdot E_i|^2 = |G_\Sigma \cdot E_i|^2 + |G_\Delta \cdot E_i|^2 \quad (17)$$

where E_i is the incident field at the antennas. It is worthwhile to note that the MRC equation (17) formulated in power quantities is equivalent to the formulation (3) in SNR quantities for the Random-LOS case, proof of which is straightforward and therefore omitted here.

The replacement vectors can be obtained by a linear transformation of the form

$$\begin{bmatrix} G_\Sigma \\ G_\Delta \end{bmatrix} = \mathbf{U} \begin{bmatrix} G_1 \\ G_2 \end{bmatrix} \quad (18)$$

where

$$\mathbf{U} = \begin{bmatrix} \sin \zeta & -e^{j\epsilon} \cos \zeta \\ \cos \zeta & e^{j\epsilon} \sin \zeta \end{bmatrix} \quad (19)$$

is a unitary matrix, i.e., $\mathbf{U}^H \mathbf{U} = \mathbf{I}$, with parameters

$$\epsilon = \angle G_1 \cdot G_2^* \quad (20)$$

$$\zeta = \frac{1}{2} \arctan \left(\frac{2|G_1 \cdot G_2^*|}{|G_1|^2 - |G_2|^2} \right). \quad (21)$$

A sketch of the derivations is given in Appendix A.

The orthogonalization matrix takes into account various important parameters of the MIMO antenna elements: (i) their phase difference is given by (20), (ii) the orthogonality of their far-field functions is given by the numerator of (21) and (iii) their power balance is given by the denominator of (21). For example, in the special case when $\epsilon = 0$ and the power balance prevails (i.e., $|G_1|^2 = |G_2|^2$), the orthogonalized patterns reduce to the well-known result of semi-sum and semi-difference of the original far-field functions.

In addition to the MRC SIMO diversity scheme, we apply this orthogonalization to the ZF MIMO multiplexing scheme too. Since the transformation is done by a unitary operator, the ZF MIMO scheme will remain the same, e.g., in terms of the powers (SNRs) of each of the bitstreams (4).

V. DERIVATION OF PoD FUNCTIONS

In this section we derive the PoD functions of a 1-bitstream SISO system, a 1-bitstream MRC SIMO diversity system and a 2-bitstream ZF-MIMO open loop multiplexing system as defined above. The PoD functions will be derived for a fixed AoA defined by the angles θ_0 and ϕ_0 in the spherical coordinate system associated with the receive (i.e., the characterized) antennas. Hence, in principle, we are deriving the PoD functions conditioned on the observation of one

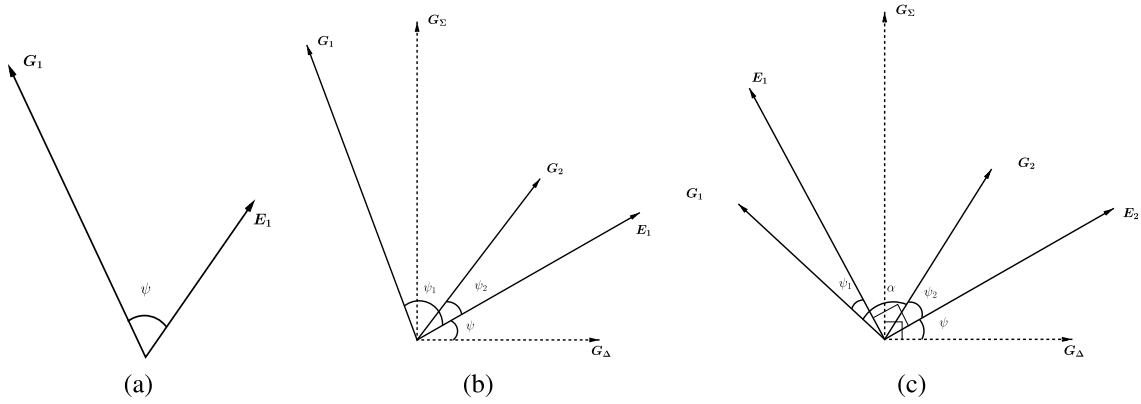


FIGURE 1. The model used for evaluation of the probability distribution of the received SNR. G_i denote the gain of the antennas while E_i denotes the impinging plane wave(s), at a defined AoA (θ_0, ϕ_0) . (a) SISO system, (b) SIMO system, and (c) 2×2 MIMO system.

or two impinging waves coming from the direction defined by (θ_0, ϕ_0) depending upon whether we are dealing with a 1- or 2-bitstream system. A schematic representation of the vectors describing the channel model used for SISO, SIMO, and MIMO systems are illustrated in Fig. 1. The polarization vectors of an impinging wave (or two orthogonally polarized waves) and the receive antenna (or antennas) is random obeying the probability distribution (15).

A. 1-BITSTREAM SISO SYSTEM

Let's consider a 1-bitstream SISO system defined by (2) and (10). Following the notation in [15], we then obtain from (10) and (14) that the SISO SNR in (2) is given by

$$\gamma = G_o(\theta_0, \phi_0) \cos^2(\psi) \gamma_t = \gamma_{\max} \cos^2(\psi) \quad (22)$$

where γ_t is the transmit SNR or equivalently, in this case, the receive SNR by a polarization-aligned isotropic antenna, $G_o(\theta_0, \phi_0)$ is the gain of the receive antenna in direction (θ_0, ϕ_0) , and $\gamma_{\max} = G_o(\theta_0, \phi_0) \gamma_t$ is the maximum SNR attained for polarization-matching at AoA (θ_0, ϕ_0) , and ψ is the angle defined by the vectors $\mathbf{G}(\theta_0, \phi_0)$ and $\mathbf{E}(\theta_0, \phi_0)$ or equivalently by the corresponding polarization vectors $\hat{\mathbf{g}}(\theta_0, \phi_0)$ and $\hat{\mathbf{e}}(\theta_0, \phi_0)$, respectively.

Assuming (15) we find the probability distribution function (PDF)² of the receive SISO SNR (22)

$$f(\gamma) = \frac{1}{\pi \sqrt{\gamma(\gamma_{\max} - \gamma)}} \quad (23)$$

where $0 \leq \gamma \leq \gamma_{\max}$. The corresponding cumulative distribution function (CDF) is then given by

$$F(\gamma) = \frac{2}{\pi} \arctan \sqrt{\frac{\gamma}{\gamma_{\max} - \gamma}}. \quad (24)$$

Derivations of (23) and (24) are provided in Appendix C.

It can be readily observed from (24), that the median SNR is $\gamma_{\max}/2$ since $F(\gamma_{\max}/2) = 1/2$, which is also the

²It is worthwhile to note that (23) in the general Random-LOS channel where the AoAs (θ_0, ϕ_0) are not fixed, but random variables, represents a conditional PDF.

average SNR. The physical interpretation is that for any SISO system the power loss in Random-LOS due to polarization mismatch is 3dB on average.

By using the ideal threshold receiver model (5), the PoD of a 1-bitstream SISO system is obtained as

$$\text{PoD}_{\text{SISO}}(\gamma_t/\gamma_{\text{th}}) = 1 - \frac{2}{\pi} \arctan \sqrt{\frac{1}{G_o \frac{\gamma_t}{\gamma_{\text{th}}} - 1}} \quad (25)$$

where $\gamma_t/\gamma_{\text{th}}$ indicates the power (relative the receiver threshold level) required to achieve a certain PoD level, and $\gamma_t/\gamma_{\text{th}} \geq 1/G_o$.

By a closer inspection of (25), we immediately see that in SISO systems operating in Random-LOS at a fixed PoD-level, a decrease in antenna gain in the desired direction will require an increase of transmit power, a better receiver sensitivity or both. Different antenna designs can be readily compared by plugging in the measured or simulated antenna gains.

B. 1-BITSTREAM MRC SIMO SYSTEM

Let's now consider the 1-bitstream SIMO system with MRC of the receive signals at the two ports of the antenna system. Combining (11) and (14) into (3) and after some straightforward manipulations we obtain the following MRC SIMO SNR

$$\gamma = \gamma_{\max,1} \cos^2(\psi_1) + \gamma_{\max,2} \cos^2(\psi_2) \quad (26)$$

where $\gamma_{\max,1} = G_{o,1}(\theta_0, \phi_0) \gamma_t$ and $\gamma_{\max,2} = G_{o,2}(\theta_0, \phi_0) \gamma_t$ are the maximum SNR attained at each receive port for polarization-matching at AoA (θ_0, ϕ_0) and γ_t is the transmit SNR. $G_{o,1}(\theta_0, \phi_0)$ and $G_{o,2}(\theta_0, \phi_0)$ are the gains of the two receive antennas in direction (θ_0, ϕ_0) . ψ_1 and ψ_2 are the corresponding polarization mismatch angles shown in Fig. 1(b).

Our aim is to derive the PoD of 1-bitstream with MRC in a SIMO system. Hence, we apply the orthogonalization transformation of the receive far-field functions shown in Sec. IV that leads to a simplification of the PoD derivations.

Indeed, after the orthogonalization (26) can be rewritten as

$$\gamma = \gamma_{\Sigma} \sin^2(\psi) + \gamma_{\Delta} \cos^2(\psi) \quad (27)$$

where $\gamma_{\Sigma} = G_{\Sigma}(\theta_0, \phi_0)\gamma_t$ and $\gamma_{\Delta} = G_{\Delta}(\theta_0, \phi_0)\gamma_t$ are the maximum SNR attained at each receive port for polarization-matching at AoA (θ_0, ϕ_0) . γ_t is the transmit SNR. $G_{\Sigma} = |\sqrt{G_{\Sigma}}\hat{\mathbf{g}}_{\Sigma}|^2$ and $G_{\Delta} = |\sqrt{G_{\Delta}}\hat{\mathbf{g}}_{\Delta}|^2$ are the gains of the two orthogonalized receive antennas in direction (θ_0, ϕ_0) . ψ is the corresponding random polarization mismatch angle (14) shown in Fig. 1(b) and satisfying the PDF (15).

The PDF of γ is then given by

$$f(\gamma) = \frac{1}{\pi \sqrt{(\gamma_{\Delta} - \gamma)(\gamma - \gamma_{\Sigma})}} \quad (28)$$

where $\min(\gamma_{\Delta}, \gamma_{\Sigma}) \leq \gamma \leq \max(\gamma_{\Delta}, \gamma_{\Sigma})$. The corresponding CDF of the received SNR is obtained as

$$F(\gamma) = \frac{1}{2} + \frac{1}{\pi} \arctan\left(\frac{2\gamma - \gamma_{\Delta} - \gamma_{\Sigma}}{2\sqrt{(\gamma_{\Delta} - \gamma)(\gamma - \gamma_{\Sigma})}}\right). \quad (29)$$

From (29) we see that the median SNR is $(\gamma_{\Delta} + \gamma_{\Sigma})/2$, i.e., the arithmetic average of the power available in the orthogonal polarizations.

Two limiting cases can be discerned here: (i) $\min(\gamma_{\Delta}, \gamma_{\Sigma}) = 0$, then (28) and (29) reduce to (23) and (24), respectively. The physical interpretation is that the antennas are co-polarized at the AoA (θ_0, ϕ_0) , (ii) $\gamma_{\Delta} = \gamma_{\Sigma}$, then (28) and (29) are not valid. The corresponding CDF and PDF (not shown here) are then given by the Dirac δ -function and the Heaviside θ -function, respectively. This can be intuitively understood from (27) since the SNR becomes independent from the polarization mismatch angle. The physical interpretation is that the receive antennas are orthogonal and power-balanced and therefore able to collect all the available energy regardless the polarization of the impinging wave.

Detailed derivations of (28) and (29) are presented in Appendix C.

The corresponding PoD of 1-bitstream MRC SIMO system is computed as

$$\text{PoD}_{\text{SIMO}}(\gamma_t/\gamma_{\text{th}}) = \frac{1}{2} - \frac{1}{\pi} \arctan\left(\frac{1 - \left(\frac{G_{\Delta} + G_{\Sigma}}{2}\right) \frac{\gamma_t}{\gamma_{\text{th}}}}{\sqrt{(G_{\Delta} \frac{\gamma_t}{\gamma_{\text{th}}} - 1)(1 - G_{\Sigma} \frac{\gamma_t}{\gamma_{\text{th}}})}}\right). \quad (30)$$

In this case the impact of the decrease of the antenna gains are not as straightforward as in the SISO case. However, we clearly see that both gains will affect the performance of the polarization diversity. It can then be evaluated by (30) and (18)-(21).

C. 2-BITSTREAM ZF MIMO SYSTEM

We now consider the 2-bitstream MIMO system with ZF applied to the received signals at the two ports of the antenna system. Similar to the MRC SIMO case, we apply the orthogonalization transformation to the receiver far-field vectors.

Here, as mentioned above, the two incoming plane waves \mathbf{E}_1 and \mathbf{E}_2 are orthogonal. Since γ_t is the same for both bitstreams, the input-output relationship (4), channel (12) and the condition of weakest stream (6) provide, after some straightforward manipulations, the following ZF MIMO SNR

$$\gamma = \min\left(\frac{C\gamma_t}{G_{\Sigma} \sin^2(\psi) + G_{\Delta} \cos^2(\psi)}, \frac{C\gamma_t}{G_{\Sigma} \cos^2(\psi) + G_{\Delta} \sin^2(\psi)}\right), \quad (31)$$

where G_{Δ} and G_{Σ} are the gains of the orthogonalized receive antennas in direction (θ_0, ϕ_0) , same as the MRC case, and ψ is the polarization mismatch angle as shown in Fig. 1(c), and

$$C = G_{o,1}(\theta_0, \phi_0)G_{o,2}(\theta_0, \phi_0) \sin^2(\alpha) \quad (32)$$

only depends on ϕ_0 and θ_0 and the gains of the receiver antennas in that direction, and is independent of the polarization mismatch. Hence, it can be considered a constant in our case. In (32), α is the angle between the two receiver antenna polarizations, as shown in Fig. 1(c).

In the same way as above, knowing the probability distribution of ψ , that of γ in (31) is derived as

$$f(\gamma) = \frac{2C\frac{\gamma_t}{\gamma}}{\pi \sqrt{G_{\Sigma}G_{\Delta}} \sqrt{\left(\frac{C\gamma_t}{G_{\Delta}} - \gamma\right)\left(\gamma - \frac{C\gamma_t}{G_{\Sigma}}\right)}} \quad (33)$$

where $\min(\frac{C\gamma_t}{G_{\Delta}}, \frac{C\gamma_t}{G_{\Sigma}}) \leq \gamma \leq \frac{2C\gamma_t}{G_{\Sigma} + G_{\Delta}}$. The CDF of the received SNR is

$$F(\gamma) = 1 - \frac{2}{\pi} \arctan\left(\frac{\frac{C}{G_{\Delta}G_{\Sigma}}\left(\frac{\gamma_t}{\gamma}\right) - \frac{1}{2}\left(\frac{1}{G_{\Delta}} + \frac{1}{G_{\Sigma}}\right)}{\frac{1}{\sqrt{G_{\Delta}G_{\Sigma}}} \sqrt{\left(\frac{C}{G_{\Sigma}} \frac{\gamma_t}{\gamma} - 1\right)\left(1 - \frac{C}{G_{\Delta}} \frac{\gamma_t}{\gamma}\right)}}\right) \quad (34)$$

Derivations of (33) and (34) are presented in Appendix C.

As in the MRC SIMO case we see that when $G_{\Delta} = G_{\Sigma}$, the above CDF and PDF are not valid and rather described by the Dirac δ -function and the Heaviside θ -function, respectively. The physical interpretation is that the receive antennas are orthogonal and power-balanced and therefore there is no interference for the two bitstreams. The antennas are able to collect all the available energy regardless the polarization of the impinging waves.

The PoD can be written as

$$\text{PoD}_{\text{MIMO}}(\gamma_t/\gamma_{\text{th}}) = \frac{2}{\pi} \arctan\left(\frac{\frac{C}{G_{\Delta}G_{\Sigma}}\left(\frac{\gamma_t}{\gamma_{\text{th}}}\right) - \frac{1}{2}\left(\frac{1}{G_{\Delta}} + \frac{1}{G_{\Sigma}}\right)}{\frac{1}{\sqrt{G_{\Delta}G_{\Sigma}}} \sqrt{\left(\frac{C}{G_{\Sigma}} \frac{\gamma_t}{\gamma_{\text{th}}} - 1\right)\left(1 - \frac{C}{G_{\Delta}} \frac{\gamma_t}{\gamma_{\text{th}}}\right)}}\right) \quad (35)$$

The performance of the ZF polarization multiplexing can then be evaluated by (35) and (18)-(21).

VI. NUMERICAL EXAMPLES

In this section we illustrate the application of the derived PoD equations in the evaluation of the MIMO performance of dual-polarized antennas. In polarization-diversity or polarization-MIMO systems, the performance is optimal if the two antenna ports provide orthogonal and equal-amplitude far-field patterns. However, it is known that the two ports of a dual-polarized antenna, will provide orthogonal and amplitude-balanced far-fields only close to boresight direction. The amplitude imbalance (I_a) and polarization non-orthogonality (I_p) which occur at AoAs away from boresight, will degrade the performance of an antenna in Random-LOS. I_a and I_p , which are collectively referred to as polarization deficiencies, are defined as

$$I_a(\theta, \phi) = \frac{\max\{|\mathbf{G}_1|, |\mathbf{G}_2|\}}{\min\{|\mathbf{G}_1|, |\mathbf{G}_2|\}}, \quad (36)$$

$$I_p(\theta, \phi) = \frac{|\mathbf{G}_1 \cdot \mathbf{G}_2^*|}{|\mathbf{G}_1| |\mathbf{G}_2|}, \quad (37)$$

where \mathbf{G}_1 and \mathbf{G}_2 are the far-field vectors of the two antenna ports. Both I_a and I_p are equal to zero for the ideal case.

In order to study the effects of the polarization deficiencies, on MRC and ZF performance of dual-polarized antennas in Random-LOS, we choose the figure of merit as the MIMO efficiency defined in [11]. The MIMO efficiency is defined as the degradation in the required SNR to achieve 95% PoD level, compared to the ideal case where the polarization deficiencies are not present, i.e.

$$\eta_{\text{MIMO}} = \frac{\text{PoD}_0^{-1}(0.95)}{\text{PoD}^{-1}(0.95)}, \quad (38)$$

where PoD^{-1} is the inverse function of PoD, and PoD_0 represents the PoD of the ideal case. For the 1-bitstream system, the definition in (38) is in fact a SIMO efficiency. However, in order to avoid multiple definitions and following the notation in [11] the term MIMO efficiency is used for both SIMO and MIMO systems.

Close inspection of (21) shows that ζ can be written in terms of I_a and I_p as

$$\zeta = \frac{1}{2} \arctan\left(\frac{2I_p}{I_a - 1/I_a}\right), \quad (39)$$

where we have assumed $|\mathbf{G}_1| > |\mathbf{G}_2|$. The MIMO efficiency of MRC and ZF systems can then be calculated for different values of the polarization deficiencies. For this purpose, (30) and (35) need to be solved for $\gamma/\gamma_{\text{th}}$ at $\text{PoD} = 0.95$, respectively for MRC and ZF cases. It should be noted that having $|\mathbf{G}_1| < |\mathbf{G}_2|$ would not affect the dependence of the MIMO efficiency on the polarization deficiencies.

Fig. 2(a) shows the degradation of the MIMO efficiency vs. I_a for a SIMO system with $I_p = 0$. Similarly, Fig. 2(b) shows the MIMO efficiency vs. I_p when $I_a = 0$ dB. The analytical MIMO efficiency is compared with the simulated values in [11] and shows the exact agreement between the analytical and simulated values.

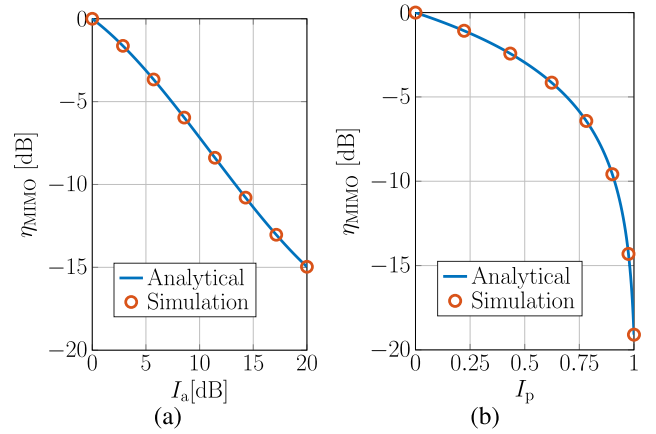


FIGURE 2. MIMO efficiency of a SIMO system vs. the polarization deficiencies (a) amplitude imbalance, and (b) polarization non-orthogonality.

In order to investigate the effect of the presence of both polarization deficiencies at the same time, the MIMO efficiency of 1-bitstream MRC system is plotted vs. the polarization deficiencies in Fig. 3(a). It is observed that the MIMO efficiency decreases in the presence of either of the two polarization deficiencies, as expected. The MIMO efficiency of 2-bitstream ZF system is plotted in Fig. 3(b) for comparison. We observe that the adverse effect of the polarization deficiencies is larger on ZF system than on MRC system, especially at I_p values close to 1, where the far-field vectors of the receiver antennas are almost parallel.

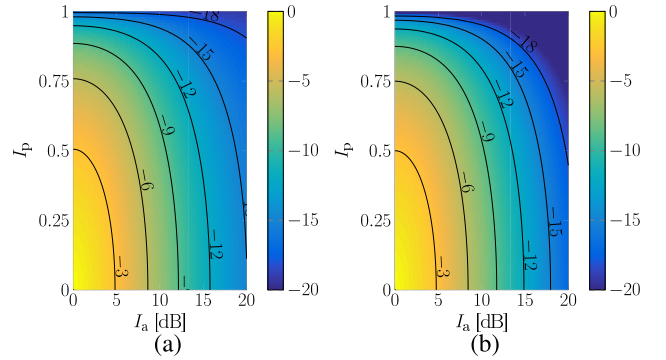


FIGURE 3. MIMO efficiency of (a) a 1-bitstream MRC system, and (b) a 2-bitstream ZF system vs. the polarization deficiencies.

These results can be readily applied to any dual-polarized antenna in order to study its performance in Random-LOS. This information is especially useful when dealing with base-station antennas for mm-wave 5G or small cells where LOS is expected to be the dominant propagation environment between the base-station and the mobile device. For such scenarios, it is essential that the antenna provides a desirable MIMO performance over the intended coverage area. Here, we use the dual-polarized self-grounded bowtie antenna [16] as an example to demonstrate the application of the derived equations in obtaining the MIMO efficiency coverage.

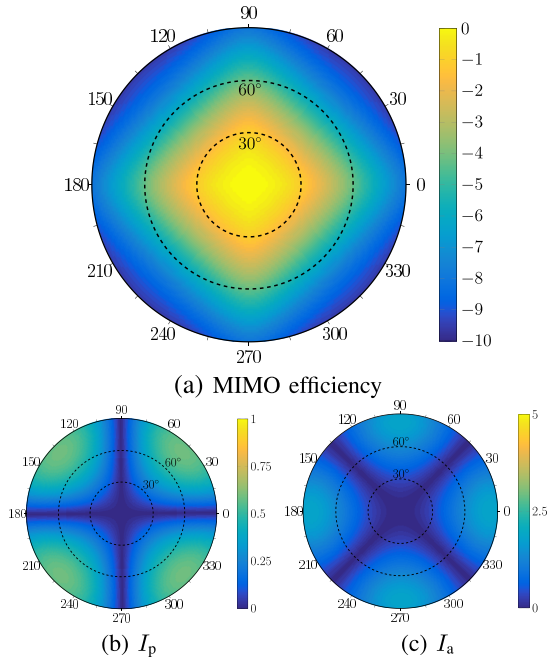


FIGURE 4. (a) The MIMO efficiency, (b) polarization non-orthogonality, and (c) amplitude imbalance in dB, of the dual-polarized self-grounded bowtie antenna at 1.6GHz.

These results can be compared to the numerically simulated ones in [17] which shows the agreement between the formulae and the simulation. Without using the derived equations, one needs to run time-consuming numerical simulations in order to obtain the efficiency, whereas the efficiency is readily available with the presented closed-form formulas.

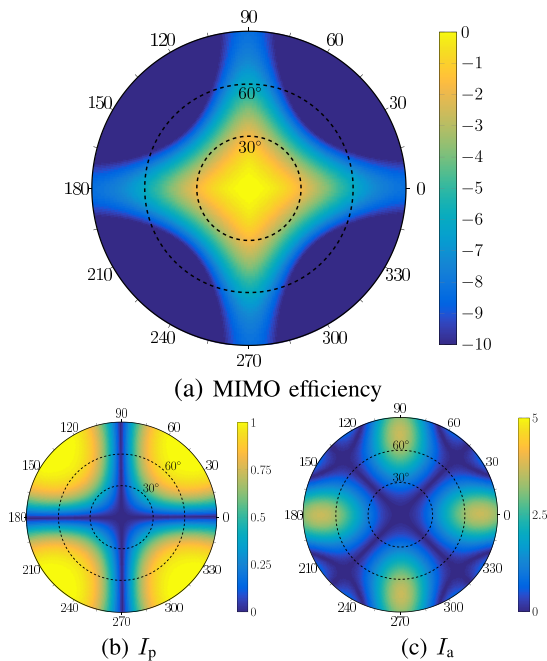


FIGURE 5. (a) The MIMO efficiency, (b) polarization non-orthogonality, and (c) amplitude imbalance in dB, of the dual-polarized self-grounded bowtie antenna at 2.2GHz.

Fig. 4(a) shows the ZF MIMO efficiency coverage of the dual-polarized self-grounded bowtie antenna in the half-space in front the antenna, at 1.6 GHz. It is observed that while the antenna provides a good 2-bitstream coverage for directions close to the boresight, at directions away from boresight more power is required at the transmitter side in order to achieve 95% PoD. Fig. 4(b) and 4(c) show the spatial distribution of the polarization deficiencies at the same frequency, where the effect of the polarization deficiencies on the MIMO efficiency coverage is seen clearly. Same functions are plotted in Fig. 5 for 2.2 GHz. It is observed that the polarization deficiencies are more pronounced at this frequency which results in poor MIMO coverage in larger portions of the space. The PoD equations (30) and (35) can be employed during the design process of dual-polarized antennas to rapidly evaluate the MIMO performance of the antenna and optimize the design, without the need for potentially complex and time-consuming numerical simulations.

VII. CONCLUSIONS

We have produced analytical expressions for the probability distribution functions of the receive signal-to-noise ratio for maximum ratio combining receiver diversity and the zero-forcing multiplexing receiver algorithms in Random-LOS environments under the assumption that angle-of-arrival of the field impinging at the receive antenna is fixed. Based on the above, the performance of different 1-bitstream and 2-bitstream communication systems are analytically studied in Random-LOS propagation environments.

As an intermediate step in the derivations we have produced a general analytical orthogonalization transformation matrix for far-field functions of arbitrary dual-polarized antennas. The relationship of the parameters of the far-field orthogonalization matrix and the effects of polarization deficiencies on the system performance are also described and formulated. For dual-polarized antennas, polarization deficiencies are present at off-boresight directions and lead to degradation in the performance of the whole system. These analytical studies help resolve the need for often time-consuming simulations and provide a better understanding of the Random-LOS propagation and the effect of polarization deficiencies of the dual-polarized receiver antenna, and also the effect of the polarization mismatch between the two ends of the communication link, on the performance of MIMO systems.

APPENDIX A SKETCH PROOF OF ORTHOGONALIZATION OF ARBITRARY FAR-FIELD VECTORS

Assume two arbitrary non-orthogonal complex vectors \mathbf{G}_1 and \mathbf{G}_2 , representing far-field functions of two antennas at a random direction. The objective is to find two vectors \mathbf{G}_Σ and \mathbf{G}_Δ that for any incident field (\mathbf{E}_i) satisfy conditions of orthogonality (16) and of conservancy of received power according to the MRC diversity scheme (17).

We now seek the vectors \mathbf{G}_Σ and \mathbf{G}_Δ as linear combinations of the original vectors

$$\begin{bmatrix} \mathbf{G}_\Sigma \\ \mathbf{G}_\Delta \end{bmatrix} = \begin{bmatrix} a & b \\ c & d \end{bmatrix} \begin{bmatrix} \mathbf{G}_1 \\ \mathbf{G}_2 \end{bmatrix} \quad (40)$$

The power equation (17) gives:

$$\begin{aligned} |(a\mathbf{G}_1 + b\mathbf{G}_2) \cdot \mathbf{E}_i^*|^2 + |(c\mathbf{G}_1 + d\mathbf{G}_2) \cdot \mathbf{E}_i^*|^2 \\ = |ah_1 + bh_2|^2 + |ch_1 + dh_2|^2 \\ = (ah_1 + bh_2)(ah_1 + bh_2)^* + (ch_1 + dh_2)(ch_1 + dh_2)^* \\ = (|a|^2 + |c|^2)|h_1|^2 + (|b|^2 + |d|^2)|h_2|^2 \\ + (ab^* + cd^*)h_1h_2^* + (a^*b + c^*d)h_1^*h_2 \\ = |h_1|^2 + |h_2|^2. \end{aligned} \quad (41)$$

It is worthwhile to note that the equality of the equations above are valid up to a multiplicative constant that has been omitted in order to improve clarity of exposition.

Equation (41) has to hold for every arbitrary incident field or h_1 and h_2 , so the weights should satisfy the following three equations:

$$|a|^2 + |c|^2 = 1, \quad (42a)$$

$$|b|^2 + |d|^2 = 1, \quad (42b)$$

$$a^*b + c^*d = 0, \quad (42c)$$

where we have to solve four unknowns. The orthogonality condition (16)

$$\mathbf{G}_\Sigma \cdot \mathbf{G}_\Delta^* = (a\mathbf{G}_1 + b\mathbf{G}_2) \cdot (c\mathbf{G}_1 + d\mathbf{G}_2)^* = 0; \quad (43)$$

provides the fourth equation

$$ac^*|\mathbf{G}_1|^2 + ad^*\mathbf{G}_1 \cdot \mathbf{G}_2^* + bc^*\mathbf{G}_2 \cdot \mathbf{G}_1^* + bd^*|\mathbf{G}_2|^2 = 0. \quad (44)$$

Equations (16) and (17) suggest that we can define intermediate unknowns v, ω, k, l, m , and n and write the weights as

$$a = e^{jk} \sin v, \quad c = e^{jm} \cos v \quad (45a)$$

$$b = e^{jl} \sin \omega, \quad d = e^{jn} \cos \omega \quad (45b)$$

By further inserting (45a)-(45b) into our system of four equations we obtain the sought results (19), (20) and (21) after some lengthy and tedious algebraic manipulations. They are therefore omitted here.

APPENDIX B SKETCH OF DERIVATION OF ZF MIMO SNR

The channel matrix of a 2×2 MIMO system is given by

$$\mathbf{H} = \begin{bmatrix} h_{11} & h_{12} \\ h_{21} & h_{22} \end{bmatrix} \quad (46)$$

Assuming the model in Fig. 1(c) and (12), the elements of \mathbf{H} can be written as

$$h_{11} = \sqrt{G_{0,1}} \cos(\psi_1) e^{-j\phi_{11}}, \quad (47a)$$

$$h_{12} = \sqrt{G_{0,1}} \sin(\psi_1) e^{-j\phi_{12}}, \quad (47b)$$

$$h_{21} = -\sqrt{G_{0,2}} \sin(\psi_2) e^{-j\phi_{21}}, \quad (47c)$$

$$h_{22} = \sqrt{G_{0,2}} \cos(\psi_2) e^{-j\phi_{22}}, \quad (47d)$$

where the phases of the complex channel matrix entries are given by $\phi_{11} = \phi_{r,1} + \phi_{t,1}$, $\phi_{12} = \phi_{r,1} + \phi_{t,2}$, $\phi_{21} = \phi_{r,2} + \phi_{t,1}$, and $\phi_{22} = \phi_{r,2} + \phi_{t,2}$. The phases $\phi_{r,i}$ and $\phi_{t,i}$ for $i = 1, 2$ denote the phases of the receive and transmit antennas of a 2×2 MIMO system in Random-LOS channel.

In order to compute the ZF output SNRs according to (4), we need to compute

$$\mathbf{H}^H \mathbf{H} = \begin{bmatrix} |h_{11}|^2 + |h_{21}|^2 & h_{11}^* h_{12} + h_{21}^* h_{22} \\ h_{11} h_{12}^* + h_{21} h_{22}^* & |h_{12}|^2 + |h_{22}|^2 \end{bmatrix} \quad (48)$$

and its inverse $(\mathbf{H}^H \mathbf{H})^{-1}$. The ZF output SNRs for 2 matrix are then given by

$$\gamma_1^{\text{ZF}} = \frac{\det(\mathbf{H}^H \mathbf{H}) \gamma_t}{|h_{12}|^2 + |h_{22}|^2}, \quad \gamma_2^{\text{ZF}} = \frac{\det(\mathbf{H}^H \mathbf{H}) \gamma_t}{|h_{11}|^2 + |h_{21}|^2} \quad (49)$$

The determinant of $\mathbf{H}^H \mathbf{H}$ is obtained as

$$\begin{aligned} \det(\mathbf{H}^H \mathbf{H}) &= (|h_{11}|^2 + |h_{21}|^2)(|h_{12}|^2 + |h_{22}|^2) \\ &\quad - (h_{11}^* h_{12} + h_{21}^* h_{22})(h_{11} h_{12}^* + h_{21} h_{22}^*) \\ &= (|h_{11}| |h_{22}| - |h_{21}| |h_{12}|)^2 \\ &= (\sqrt{G_{0,1}} \sqrt{G_{0,2}})^2 [\cos(\psi_1) \cos(\psi_2) \\ &\quad + \sin(\psi_1) \sin(\psi_2)]^2 \\ &= G_{0,1} G_{0,2} \sin^2(\alpha) = C, \end{aligned} \quad (50)$$

which is independent of the random polarization mismatch ψ . In the derivation of (50) we have used $\text{Im}\{h_{11}^* h_{12} h_{21} h_{22}^*\} = 0$, and $\psi_2 - \psi_1 = \pi/2 - \alpha$, which are both straightforward to prove and therefore omitted here. The denominators of (49) are similar to MRC combining of the incoming waves. Hence, the ZF receive SNRs given by (31) are now directly obtained using (50) and the orthogonalized vectors \mathbf{G}_Σ and \mathbf{G}_Δ in (4).

APPENDIX C DERIVATIONS OF PoD FUNCTIONS

The receive SNR γ is a function of polarization mismatch angle ψ

$$\gamma = g(\psi) \quad (51)$$

where ψ is a random variable with PDF (15). The PDF of γ is then obtained from the fundamental theorem [18]

$$f(\gamma) = \sum_{\psi_i} \left. \frac{f_\Psi(\psi)}{\left| \frac{d\gamma}{d\psi} \right|} \right|_{\psi_i = g^{-1}(\gamma)}, \quad (52)$$

where ψ_i are the roots of (51).

The computation of the PoDs involve the computation of integrals obtained with Wolfram integrator tool available online [19].

A. 1-BITSTREAM SISO SYSTEM

Using (15) we can write

$$\begin{aligned}
 f(\gamma) &= \frac{f_{\Psi}(\psi)}{\left| \frac{d\gamma}{d\psi} \right|} \bigg|_{\psi=\arccos \sqrt{\gamma/\gamma_{\max}}} \\
 &= \frac{\frac{2}{\pi}}{|2\gamma_{\max} \sin \psi \cos \psi|} \bigg|_{\psi=\arccos \sqrt{\gamma/\gamma_{\max}}} \\
 &= \frac{1}{\pi \sqrt{(\gamma_{\max} - \gamma)\gamma}}. \quad (53)
 \end{aligned}$$

Now considering the fact that $0 \leq \gamma \leq \gamma_{\max}$, the CDF of the received SNR can be written as

$$\begin{aligned}
 F(\gamma) &= \int_{-\infty}^{\gamma} f(\xi) d\xi = \int_0^{\gamma} \frac{1}{\pi \sqrt{\gamma_{\max} - \xi} \sqrt{\xi}} d\xi \\
 &= \frac{2}{\pi} \left[\arctan \sqrt{\frac{\xi}{\gamma_{\max} - \xi}} \right]_{\xi=0}^{\gamma} \\
 &= \frac{2}{\pi} \arctan \sqrt{\frac{\gamma}{\gamma_{\max} - \gamma}} \\
 &= \frac{2}{\pi} \arctan \sqrt{\frac{1}{\gamma_{\max}/\gamma - 1}}. \quad (54)
 \end{aligned}$$

B. 1-BITSTREAM MRC SIMO SYSTEM

Given (27) and (52), the probability distribution of the MRC combined SNR can be expressed as

$$\begin{aligned}
 f(\gamma) &= \frac{f_{\Psi}(\psi)}{\left| \frac{d\gamma}{d\psi} \right|} \bigg|_{\psi=\arccos \sqrt{\frac{\gamma-\gamma_{\Sigma}}{\gamma_{\Delta}-\gamma_{\Sigma}}}} \\
 &= \frac{\frac{2}{\pi}}{|-2(\gamma_{\Delta} - \gamma_{\Sigma}) \sin \psi \cos \psi|} \bigg|_{\psi=\arccos \sqrt{\frac{\gamma-\gamma_{\Sigma}}{\gamma_{\Delta}-\gamma_{\Sigma}}}} \\
 &= \frac{1}{\pi |-(\gamma_{\Delta} - \gamma_{\Sigma}) \sqrt{1 - \frac{\gamma-\gamma_{\Sigma}}{\gamma_{\Delta}-\gamma_{\Sigma}}} \sqrt{\frac{\gamma-\gamma_{\Sigma}}{\gamma_{\Delta}-\gamma_{\Sigma}}}|} \\
 &= \frac{1}{\pi \sqrt{(\gamma_{\Delta} - \gamma)(\gamma - \gamma_{\Sigma})}}. \quad (55)
 \end{aligned}$$

Now considering that $\min(\gamma_{\Delta}, \gamma_{\Sigma}) \leq \gamma \leq \max(\gamma_{\Delta}, \gamma_{\Sigma})$, the CDF of the received SNR is obtained as

$$\begin{aligned}
 F(\gamma) &= \int_{-\infty}^{\gamma} f(\xi) d\xi \\
 &= \frac{1}{\pi} \left[\arctan \left(\frac{2\xi - \gamma_{\Delta} - \gamma_{\Sigma}}{2\sqrt{(\gamma_{\Delta} - \xi)(\xi - \gamma_{\Sigma})}} \right) \right]_{\xi=\min(\gamma_{\Delta}, \gamma_{\Sigma})}^{\gamma} \\
 &= \frac{1}{2} + \frac{1}{\pi} \arctan \left(\frac{2\gamma - \gamma_{\Delta} - \gamma_{\Sigma}}{2\sqrt{(\gamma_{\Delta} - \gamma)(\gamma - \gamma_{\Sigma})}} \right). \quad (56)
 \end{aligned}$$

C. 2-BITSTREAM ZF MIMO SYSTEM

Close inspection of the dependence of γ on ψ shows that the probability distribution can be broken into 2 regions $\psi \in [0, \pi/2]$. The number of roots of (31) in $\psi \in [0, \pi/2]$ is

also 2. Furthermore, using symmetry, (52) is expanded as

$$\begin{aligned}
 f(\gamma) &= 2 \frac{f_{\Psi}(\psi)}{\left| \frac{d\gamma}{d\psi} \right|} \bigg|_{\psi=\arccos \sqrt{\frac{C\gamma_{\Delta} - G_{\Delta}}{G_{\Sigma} - G_{\Delta}}}} \\
 &= \frac{2C\frac{\gamma_{\Delta}}{\gamma}}{\pi \sqrt{G_{\Sigma} G_{\Delta}} \sqrt{\left(\frac{C\gamma_{\Delta}}{G_{\Delta}} - \gamma \right) \left(\gamma - \frac{C\gamma_{\Delta}}{G_{\Sigma}} \right)}}. \quad (57)
 \end{aligned}$$

Now, considering $\min(\frac{C\gamma_{\Delta}}{G_{\Delta}}, \frac{C\gamma_{\Delta}}{G_{\Sigma}}) \leq \gamma \leq \frac{2C\gamma_{\Delta}}{G_{\Sigma} + G_{\Delta}}$, the CDF of the received SNR is given as

$$\begin{aligned}
 F(\gamma) &= \int_{-\infty}^{\gamma} f_{P_1}(\xi) d\xi = \int_{\min(\frac{C\gamma_{\Delta}}{G_{\Delta}}, \frac{C\gamma_{\Delta}}{G_{\Sigma}})}^{\gamma} f(\xi) d\xi \\
 &= 1 - \frac{2}{\pi} \arctan \left(\frac{\frac{C}{G_{\Delta} G_{\Sigma}} \left(\frac{\gamma_{\Delta}}{\gamma} \right) - \frac{1}{2} \left(\frac{1}{G_{\Delta}} + \frac{1}{G_{\Sigma}} \right)}{\frac{1}{\sqrt{G_{\Delta} G_{\Sigma}}} \sqrt{\left(\frac{C}{G_{\Sigma}} \frac{\gamma_{\Delta}}{\gamma} - 1 \right) \left(1 - \frac{C}{G_{\Delta}} \frac{\gamma_{\Delta}}{\gamma} \right)}} \right). \quad (58)
 \end{aligned}$$

ACKNOWLEDGMENT

A. Razavi was with the Signals and Systems Department, Chalmers University of Technology, Gothenburg, Sweden.

REFERENCES

- [1] A. A. Glazunov, V.-M. Kolmonen, and T. Laitinen, "MIMO over-the-air testing," in *LTE-Advanced and Next Generation Wireless Networks: Channel Modelling and Propagation*. New York, NY, USA: Wiley, 2012, pp. 411–441.
- [2] M. K. Samimi and T. S. Rappaport, "3-D millimeter-wave statistical channel model for 5G wireless system design," *IEEE Trans. Microw. Theory Techn.*, vol. 64, no. 7, pp. 2207–2225, Jul. 2016.
- [3] S. Hur *et al.*, "Proposal on millimeter-wave channel modeling for 5G cellular system," *IEEE J. Sel. Topics Signal Process.*, vol. 10, no. 3, pp. 454–469, Apr. 2016.
- [4] P.-S. Kildal and J. Carlsson, "New approach to OTA testing: RIMP and pure-LOS reference environments & a hypothesis," in *Proc. 7th Eur. Conf. Antennas Propag. (EuCAP)*, Gothenburg, Sweden, Apr. 2013, pp. 315–318.
- [5] P. S. Kildal, C. Orlenius, and J. Carlsson, "OTA testing in multipath of antennas and wireless devices with MIMO and OFDM," *Proc. IEEE*, vol. 100, no. 7, pp. 2145–2157, Jul. 2012.
- [6] T. S. Rappaport *et al.*, "Millimeter wave mobile communications for 5G cellular: It will work!" *IEEE Access*, vol. 1, pp. 335–349, May 2013.
- [7] P.-S. Kildal, "Rethinking the wireless channel for OTA testing and network optimization by including user statistics: RIMP, pure-LOS, throughput and detection probability," in *Proc. Int. Symp. Antennas Propag. (ISAP)*, Nanjing, China, Oct. 2013, pp. 1–4.
- [8] P.-S. Kildal *et al.*, "Threshold receiver model for throughput of wireless devices with MIMO and frequency diversity measured in reverberation chamber," *IEEE Antennas Wireless Propag. Lett.*, vol. 10, pp. 1201–1204, 2011.
- [9] D. C. Cox, "Antenna diversity performance in mitigating the effects of portable radiotelephone orientation and multipath propagation," *IEEE Trans. Commun.*, vol. COM-31, no. 5, pp. 620–628, May 1983.
- [10] S. A. Bergmann and H. W. Arnold, "Polarisation diversity in portable communications environment," *Electron. Lett.*, vol. 22, no. 11, pp. 609–610, May 1986.
- [11] A. Razavi, A. A. Glazunov, P.-S. Kildal, and J. Yang, "Characterizing polarization-MIMO antennas in random-LOS propagation channels," *IEEE Access*, vol. 4, pp. 10067–10075, 2016.
- [12] S. M. Moghaddam, A. A. Glazunov, P.-S. Kildal, J. Yang, and M. Gustafsson, "Improvement of an octave bandwidth bowtie antenna design based on the analysis of a MIMO efficiency metric in random-LOS," *Microw. Opt. Technol. Lett.*, vol. 59, no. 6, pp. 1229–1233, 2017.

- [13] A. Razavi, A. A. Glazunov, P.-S. Kildal, and J. Yang, "Investigation of polarization deficiencies in SIMO systems in random-LOS propagation channels," in *Proc. Int. Symp. Antennas Propag. (ISAP)*, Hobart, TAS, Australia, Nov. 2015, pp. 1–3.
- [14] P.-S. Kildal, X. Chen, M. Gustafsson, and Z. Shen, "MIMO characterization on system level of 5G microbase stations subject to randomness in LOS," *IEEE Access*, vol. 2, pp. 1064–1077, Sep. 2014.
- [15] P.-S. Kildal. (2015). *Foundations of Antennas: A Unified Approach for Line-of-Sight and Multipath*. Kildal Antenn AB. [Online]. Available: <http://www.kildal.se>
- [16] H. Raza, A. Hussain, J. Yang, and P.-S. Kildal, "Wideband compact 4-port dual polarized self-grounded bowtie antenna," *IEEE Trans. Antennas Propag.*, vol. 62, no. 9, pp. 4468–4473, Sep. 2014.
- [17] S. M. Moghaddam, A. A. Glazunov, J. Yang, M. Gustafsson, and P.-S. Kildal, "Comparison of 2-bitstream polarization-MIMO performance of 2 and 4-port bowtie antennas for LTE in random-LOS," in *Proc. Int. Symp. Antennas Propag. (ISAP)*, Hobart, TAS, Australia, Nov. 2015, pp. 1–4.
- [18] S. Miller and D. Childers, *Probability and Random Processes: With Applications to Signal Processing and Communications*. San Diego, CA, USA: Academic, 2012.
- [19] (2016). *Integral Calculator: Integrate with Wolfram/Alpha*. Accessed: Jul. 2016. [Online]. Available: <http://integrals.wolfram.com/>



AIDIN RAZAVI received the M.Sc. degree in microwave engineering from Tarbiat Modares University, Tehran, Iran, in 2007, and the Swedish Licentiate and Ph.D. degrees from the Chalmers University of Technology, Gothenburg, Sweden, in 2014 and 2016, respectively. From 2007 to 2009, he was with Hamrah Telecom Company, Iran, as a Senior Engineer. From 2009 to 2011, he was with Huawei Technologies Company, as a Radio Network Planning and Optimization Engineer. He is currently a Research Engineer with Ericsson Research, Gothenburg. His research interests include OTA measurements, 5G systems, random line-of-sight propagation, MIMO systems, near-field radiation, and optimal antenna apertures.



ANDRÉS ALAYÓN GLAZUNOV (SM'11) was born in Havana, Cuba, in 1969. He received the M.Sc. (Engineer-Researcher) degree in physical engineering from Peter the Great St. Petersburg Polytechnic University, Russia, in 1994, and the Ph.D. degree in electrical engineering from Lund University, Sweden, in 2009. He has held various research and specialist positions in industry, e.g., Ericsson Research, Telia Research, and TeliaSonera, all in Sweden, from 1996 to 2005.

From 2001 to 2005, he was the Swedish Delegate to the European Cost Action 273 and was active in the Handset Antenna Working Group. He has been one of the pioneers in establishing OTA measurement techniques. He has contributed to European research projects, and to the international 3GPP and the ITU standardization bodies. From 2009 to 2010, he held a Marie Curie Senior Research Fellowship at the Centre for Wireless Network Design, University of Bedfordshire, U.K. From 2010 to 2014, he held a post-doctoral position with the Electromagnetic Engineering Laboratory, KTH-Royal Institute of Technology, Stockholm, Sweden.

Dr. Glazunov is currently an Assistant Professor with the Communications and Antenna Systems Division, Department of Electrical Engineering, Chalmers University of Technology, Gothenburg, Sweden. He is the author of more than hundred scientific and technical publications. He is the co-author and co-editor of the book titled *LTE-Advanced and Next Generation Wireless Networks* (Wiley, 2012). His current research interests include, but are not limited to electromagnetic theory, fundamental limitations on antenna-channel interactions, RF propagation channel measurements, modeling and simulations, and the OTA characterization of antenna systems and wireless devices.

...